Compensatory enlargement of Ossabaw miniature swine coronary arteries in diffuse atherosclerosis

CrossMark

Jenny S. Choy [a], Tong Luo [a], Yunlong Huo [a], Thomas Wischgoll [b], Kyle Schultz [c], Shawn D. Teague [d], Michael Sturek [c], Ghassan S. Kassab [a,c,e,*]

[a] Department of Biomedical Engineering, Indiana University Purdue University Indianapolis, Indianapolis, IN, United States
[b] Department of Computer Science and Engineering, Wright State University, Dayton, OH, United States
[c] Department of Cellular and Integrative Physiology, Indiana University, Indianapolis, IN, United States
[d] Department of Radiology, Indiana University, Indianapolis, IN, United States
[e] Department of Surgery, Indiana University, Indianapolis, IN, United States

ARTICLE INFO

ABSTRACT

Studies in human and non-human primates have confirmed the compensatory enlargement or positive remodeling (Glagov phenomenon) of coronary vessels in the presence of focal stenosis. To our knowledge, this is the first study to document arterial enlargement in a metabolic syndrome animal model with diffuse coronary artery disease (DCAD) in the absence of severe focal stenosis. Two different groups of Ossabaw miniature pigs were fed a high fat atherogenic diet for 4 months (Group I) and 12 months (Group II), respectively. Group I (6 pigs) underwent contrast enhanced computed tomographic angiography (CCTA) and intravascular ultrasound (IVUS) at baseline and after 4 months of high fat diet, whereas Group II (7 pigs) underwent only IVUS at 12 months of high fat diet. IVUS measurements of the left anterior descending (LAD), left circumflex (LCX) and right coronary (RCA) arteries in Group I showed an average increase in their lumen cross-sectional areas (CSA) of 25.8%, 11.4%, and 43.4%, respectively, as compared to baseline. The lumen CSA values of LAD in Group II were found to be between the baseline and 4 month values in Group I. IVUS and CCTA measurements showed a similar trend and positive correlation. Fractional flow reserve (FFR) was 0.91 ± 0.07 at baseline and 0.93 ± 0.05 at 4 months with only 2.2%, 1.6% and 1% stenosis in the LAD, LCX and RCA, respectively. The relation between percent stenosis and lumen CSA shows a classical Glagov phenomenon in this animal model of DCAD.

© 2014 The Authors. Published by Elsevier Ireland Ltd. This is an open access article under the CC BY-NC-ND license (http://creativecommons.org/licenses/by-nc-nd/3.0/).

1. Introduction

Post-mortem and in vivo studies suggest that coronary artery diameter increases as a consequence of atherosclerosis [1–7]. This phenomenon, also known as the Glagov phenomenon, is characterized by an outward enlargement of the vessel wall (positive remodeling) without compromise of the lumen area during the early stages of atherosclerosis [2]. It has also been reported [2] that the capacity for compensatory positive remodeling ceases when the plaque occupies approximately 40% of the potential lumen area. The phenomenon was described in a histological autopsy study twenty five years ago [2] and has since been demonstrated in vivo in humans using intravascular ultrasound (IVUS) [1,3,5,7,8], epicardial echocardiogram [4], and contrast enhanced tomographic angiography (CCTA) [6].

It is generally accepted that coronary atherosclerosis is a geometrically focal and eccentric disease [9], and that coronary lesions evolve in an independent manner [10]. Hemodynamic forces regulate vascular structure, as well as influence the development of atherosclerosis and other pathologies [11–13]. Several studies [11–14] on wall shear stress (WSS) have provided new insights into the contribution of the endothelium to the development of coronary artery disease and vascular remodeling.

The purpose of this atherosclerosis progression study was to assess the presence of coronary arterial enlargement during the early stages of the disease in a metabolic syndrome Ossabaw swine model known to develop both diffuse and focal coronary artery disease [15].

2. Methods

2.1. Animal model and study design

All animal experiments were performed in accordance with national and local ethical guidelines, including the Principles of Laboratory Animal Care, the Guide for the Care and Use of Laboratory Animals [16] and the National Association for Biomedical Research [17], and an

---

* Corresponding author at: The California Medical Innovations Institute, 11107 Roselle St, San Diego, CA 92121, United States. Tel.: +1 858 249 7418; fax: +1 858 249 7419.
  E-mail address: gkassab@calmi2.org (G.S. Kassab).

approved Indiana University Purdue University Indianapolis IACUC protocol regarding the use of animals in research.

Thirteen 9-month-old Ossabaw miniature pigs of either sex were divided into 2 groups. The Ossabaw body weight at baseline was 41.7 ± 1.9 kg, 74.2 ± 4.3 kg at 4 months, and 116.8 ± 8.6 kg after 12 months of high fat atherogenic diet [18]. The diet was composed of 6% to 8% kcal from proteins, 19% kcal from complex carbohydrates, and 46% to 75% kcal from hydrogenated soy bean oil (predominantly trans fatty acids), and 2% cholesterol and 0.7% cholate by weight [18]. Six Ossabaw pigs (Group I) were fed 3200 kcal daily for 4 months, and seven Ossabaw pigs (Group II) were fed the same diet for 12 months, until they were euthanized. Five 4-month-old body weight-matched Yorkshire domestic pigs (Group III), of either sex, that were fed with a lean diet for 4 months were used as the control group because Ossabaw miniature pigs do not grow when fed a lean diet [19]. The pigs were housed and fed in individual pens and had ad libitum access to water. A room temperature of 68–72 °F and humidity of 30% to 70% were maintained.

At a scheduled time, the pigs were fasted overnight. Surgical anesthesia was induced with TKX (telazol 10 mg/kg, ketamine 5 mg/kg, xylazine 5 mg/kg) and maintained with isoflurane 2–4%. Ventilation with 100% O_2 was provided with a respirator and maintained PCO_2 at approximately 35 mmHg. Electrocardiographic (ECG) leads were attached to the swine limbs. Body temperature was kept at 37.5 °C–38 °C and pH at 7.4 ± 0.1.

2.2. Imaging procedures

- Contrast enhanced computed tomographic angiography (CCTA)
CCTA is a clinically used modality that allows the identification of coronary lesions with excellent accuracy. CCTA scans were obtained by a cardiovascular radiologist at baseline and at 4 months (Group I) on a 64 detector computed tomography system (Philips Brilliance 64, Cleveland, OH). Images were acquired with a slice thickness of 0.625 mm and a reconstruction interval of 0.3 mm. The rotation time was 0.4 s with a pitch of 0.2, 120 kVp, and 1050 mAs. A XCB filter was used for reconstructions. The images were reconstructed at 5%, 15%, 25% … 75%, 85% and 95% of the R–R interval. The scan was performed during end-inspiratory breath-hold using retrospective ECG-gating. Intravenous lidocaine hydrochloride (60 μg/kg/min) and metoprolol (5 mg every minute up to a maximum dose of 25 mg) were administered to maintain the heart rate below 60 beats per minute. An intravenous injection of nitroglycerin (1.5 mg) was slowly administered to cause coronary vasodilation. Coronary arterial image acquisition was performed using 60–80 mL (3.5 to 5 mL/s) of intravenous contrast material (Isovue-370) followed by 100 mL of normal saline flush.

- CCTA imaging analysis
Image segmentation of CT data was used to extract the main trunks of the LAD, LCX and RCA by a previously validated algorithm developed by our group [20]. The segmentation data contained the central line coordinate and diameter. Since some of the image segmentation required manual operation on the more complex structures, preprocessing and post-processing were introduced to reduce the manual load and to improve the accuracy. These processes included simple segmentation of surrounding regions and 3-D edit of visualized objects. The segmented vessels were binarized and then processed by isosurface rendering. Once the 3-D visualization functions were completed in Matlab, the vessel surface was represented by triangle mesh and saved as STL files. MeshLab [21] was used to view the 3-D coronary tree and refine the structure. The list of faces and vertices in the STL file was then converted into typical patch structures to provide the spatial connectedness in terms of faces and vertices, where faces were the index of three vertices in one triangle, and vertices were the X, Y, Z coordinate of each vertex.

The lumen cross-sectional area (CSA) was determined by computation of the intersection of a plane with the vessel surface. The surface was defined by a set of vertices connected by faces forming the surface. The intersection plane was defined by a point and a normal vector. The point lied on the central line and the normal vector pointed to the direction of a pair of continuous points along the central line. The lumen CSA was obtained by calculating intersection segments of triangle patches of the vessel surface with the plane. All calculated segments were linked to each other to form a continuous intersection region. The lumen CSA measurements included in the analysis were taken every 5 mm along the length of the coronary vessels, starting at the ostium, once the entire vessel was reconstructed. Anatomical landmarks such as vessel branches were used to overlap the position of each section to the position determined by IVUS.

- Intravascular ultrasound (IVUS)
IVUS is a catheter-based technique that provides tomographic images perpendicular to the length of the coronary arteries. It provides important information regarding plaque composition and distribution. IVUS also provides vessel and lumen diameters that are fundamental in the evaluation of a coronary lesion. Coronary angiography and IVUS imaging were performed by a trained physician following standard procedures of clinical practice at baseline and at 4 months (Group I), and at 12 months (Group II). The femoral artery was cannulated with a 7 Fr introducer sheath and after full anticoagulation with heparin (100 IU/kg), a 6 Fr guiding catheter (Mach 1, HS SH, Boston Scientific, MA) was advanced over a 0.035″ guide wire into the selected coronary artery (LAD, LCX and RCA). The animals received 200 μg of intracoronary nitroglycerin before advancing the IVUS catheter. A 3.6 Fr, 40-MHz coronary imaging catheter (Atlantis SR Pro, Boston Scientific, MA) was advanced over a 0.014″ guide wire and positioned in the lumen of the distal portion of the artery where the vessel had a diameter of approximately 1.5 mm. An automatic and continuous pullback (0.5 mm/s) was performed from the distal position to the proximal portion, allowing visualization of the entire length of the coronary artery. IVUS images were recorded on S-VHS videotape, digitized and analyzed off-line using NIS-Elements AR 3.2 software (Nikon, Japan).

- IVUS imaging analysis
Still pictures from the digitized images were taken every 5 mm along the length of the coronary arteries starting at the ostium. The position along the vessel was normalized with respect to the total length, and the results were expressed in terms of the fractional longitudinal position, ranging from 0 (most proximal, at inlet of coronary artery) to 1 (vessel diameter of about 1.5 mm). The same normalization process was applied to the CCTA images to make sure that the same vessel length was used for the analysis of both IVUS and CCTA images. IVUS landmarks such as side branches were used in matching the sites of the baseline and 4 month images, and to overlap the sections measured with IVUS to the sections measured with CCTA. Frames during the diastolic phase of the cardiac cycle were used for measurements. Using the NIS-Elements software a calibration was performed by measuring 1-mm grid marks encoded in the IVUS image. Manual planimetry was used to trace the leading edges of the luminal border. The lumen CSA and the diameter of each segment were calculated.

- Hemodynamic studies
Immediately after IVUS imaging, a 0.014″ pressure/flow (combo) guide wire (Volcano Corporation, Rancho Cordova, CA) was calibrated and introduced into the guiding catheter. The wire was advanced up to the tip of the guiding catheter, where the pressure measured through the guiding catheter was verified to be equal to the pressure measured by the combo wire. The combo wire was then advanced into the coronary artery and intracoronary adenosine (120 μg) was administered to achieve steady-state hyperemia. Fractional Flow Reserve (FFR) was measured during maximal hyperemia. Recordings were taken at the distal, middle and proximal portions of the coronary arteries. A FFR value of ≤0.80 was considered flow limiting.

2.3. Statistical analysis

The data were expressed as means ± 1SD. Statistical significance of the results was assessed using SigmaStat software (Systat Software, Point Richmond, CA). The differences were evaluated with student's t-test or two-way ANOVA, where appropriate. The Siegel–Tukey test (non-parametric test) was also used to confirm the statistical analysis. $p < 0.05$ was considered statistically significant.

3. Results

The lumen CSA data in Group I correspond to measurements performed at the beginning of the study (before the atherogenic diet was initiated, i.e., baseline) and after 4 months of atherogenic diet in the same animals for LAD, LCX and RCA. When the baseline IVUS measurements were compared to the 4 month measurements there was an average (over the length of the vessel; LAD 70 ± 3.73 mm, LCX

51.3 ± 3.21 mm, and RCA 86.3 ± 4.63 mm) increase in the lumen area from 5.8 ± 2.2 mm^2 to 7.2 ± 2.3 mm^2 ($p = 0.006$) in the LAD (Fig. 1A), from 4.1 ± 1.0 mm^2 to 4.5 ± 1.0 mm^2 ($p = 0.21$) in the LCX (Fig. 1B), and from 5.5 ± 0.7 mm^2 to 7.9 ± 1.1 mm^2 ($p = 4.05E\text{-}09$) in the RCA (Fig. 1C).

The lumen area of the LAD artery at baseline and at 4 months (Group I) was compared to the lumen area of the LAD from the animals on atherogenic diet for 12 months (Group II). The CSA values at 12 months were 11.8% smaller when compared to the 4 months lumen area (6.3 ± 1.5 mm^2 vs. 7.2 ± 2.3 mm^2, $p = 0.22$, Fig. 1A) probably due to the higher percent stenosis (0 to 61.3%) at 12 months.

The lumen area of the LAD and RCA arteries (the two main coronaries that showed the most significant positive remodeling) from Group I at 4 months was compared to the lumen area of Group III. The CSA values of the LAD from fractional longitudinal position 0 to 0.5 were very similar in both groups ($p = 0.5$), whereas the values from fractional longitudinal position 0.6 to 1 were significantly larger in Group I ($p = 0.001$), Fig. 2A. The same was found in the RCA ($p = 0.5$ and $p = 0.03$, respectively), Fig. 2B. Our study shows significant positive remodeling in the distal portions of the coronary arteries as compared to the most proximal portions in the main trunks.

Fig. 3A and B show the CCTA reconstructed LAD and LCX trunks in one representative animal from Group I at baseline (Fig. 3A) and at 4 months (Fig. 3B). Based on these CCTA images, the lumen CSA was determined for Group I, as summarized in Fig. 3C and D. The CCTA lumen CSA increased from 5.2 ± 0.5 mm^2 to 7.7 ± 1.0 mm^2 ($p = 1.39E\text{-}05$) in the LAD (Fig. 3C), and from 4.4 ± 0.6 mm^2 to 5.2 ± 0.3 mm^2 ($p = 0.09$) in the LCX (Fig. 3D).
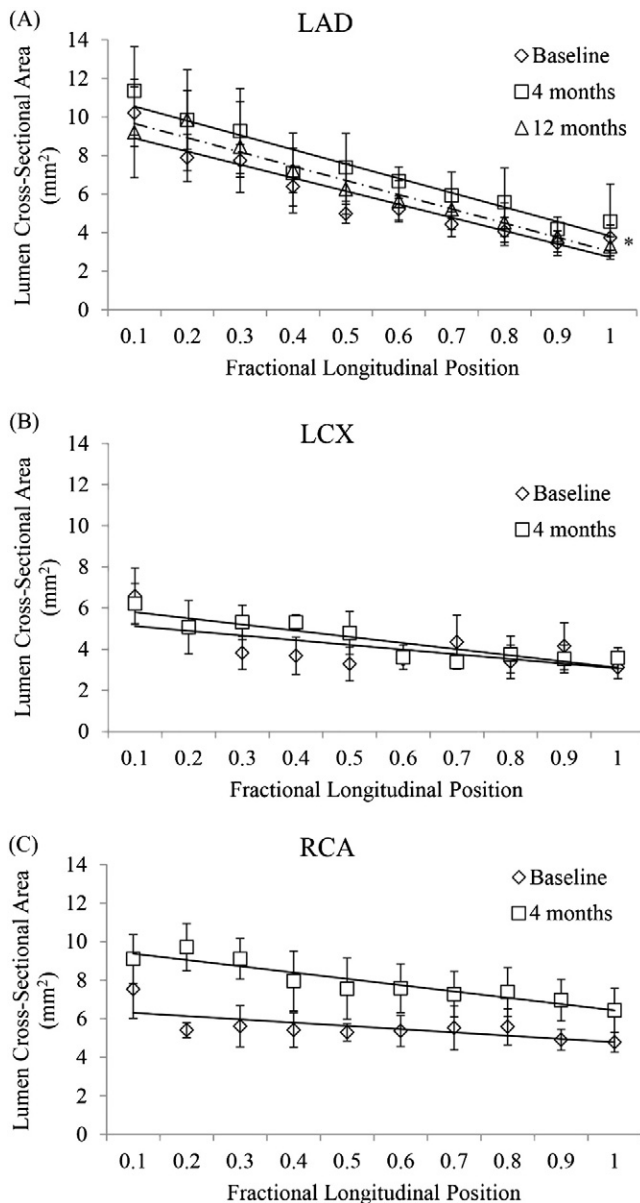
Fig. 1. A) IVUS lumen CSA of LAD artery of Ossabaw pigs at baseline, 4 months and 12 months of atherogenic diet. B) IVUS lumen CSA of LCX of Ossabaw pigs at baseline and 4 months of atherogenic diet. C) IVUS lumen CSA of RCA of Ossabaw pigs at baseline and 4 months of atherogenic diet. The data is expressed as mean ± 1SD.
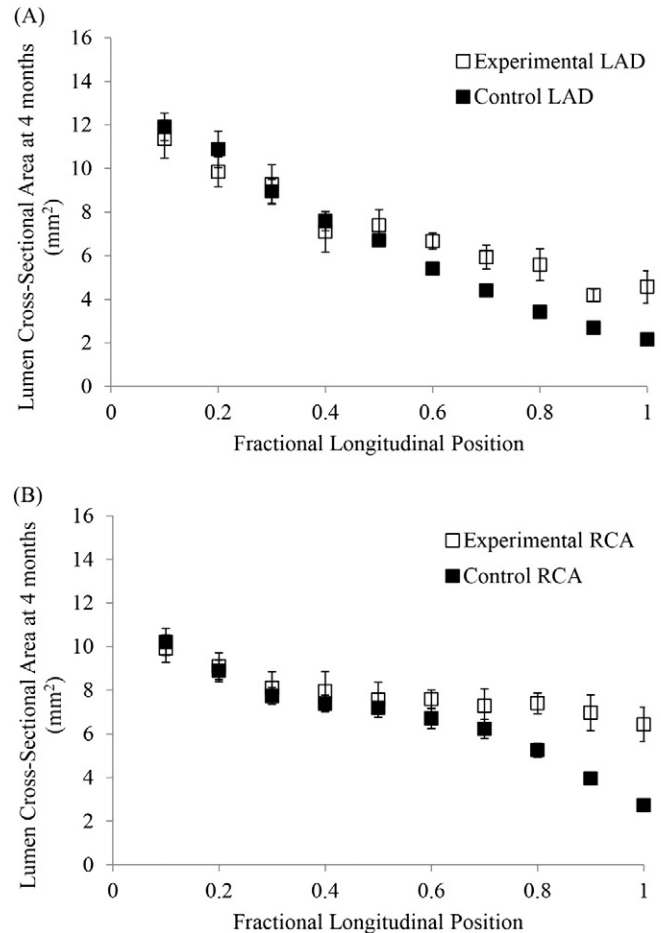
Fig. 2. Lumen CSA at 4 months from six Ossabaw (atherogenic diet) and five Yorkshire (lean diet) pigs in A) LAD and B) RCA coronary arteries. The data is expressed as mean ± 1SD.
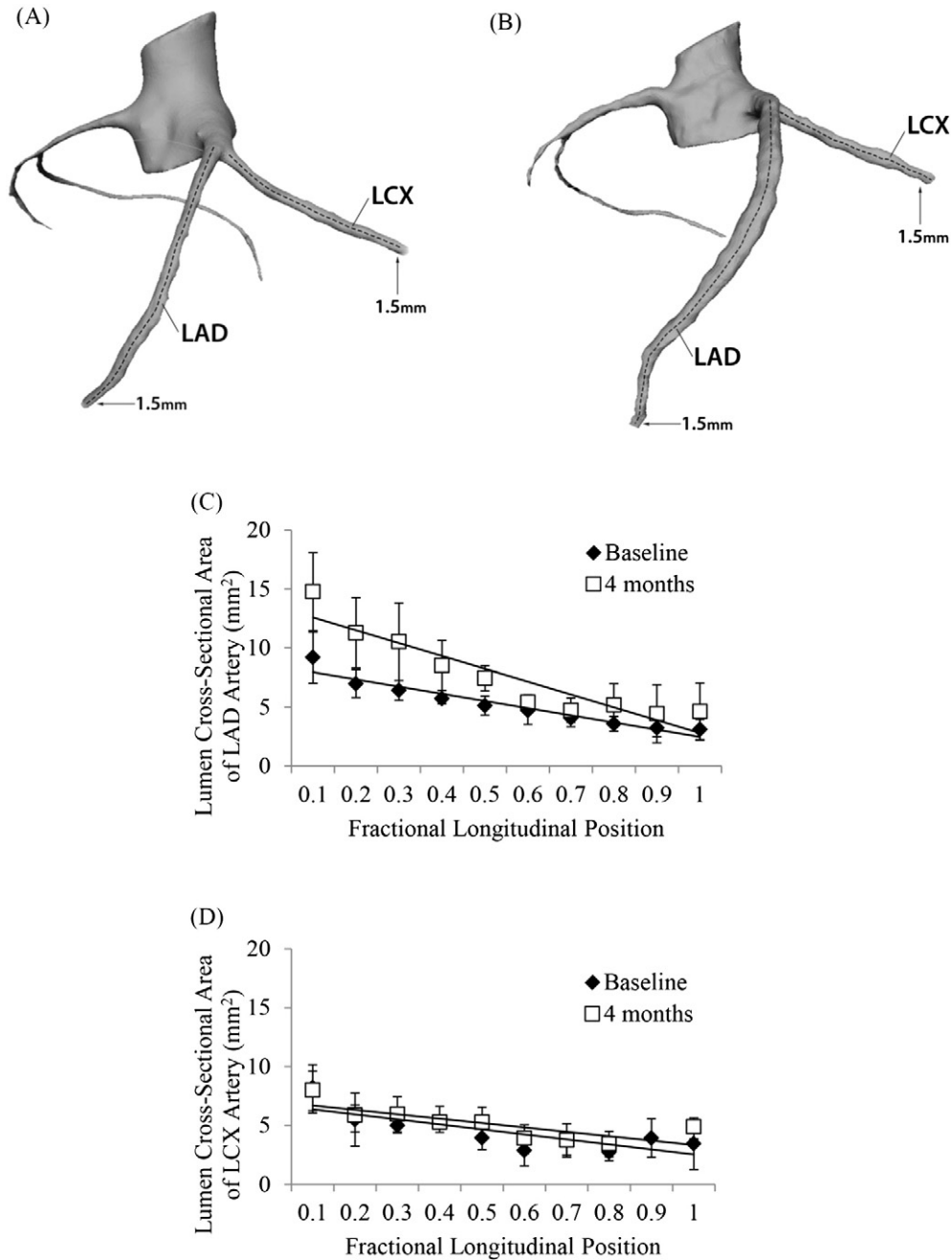
Fig. 3. LAD and LCX trunk reconstruction with center lines from one representative Ossabaw pig from CCTA images at A) baseline and B) 4 months. CCTA lumen CSA from six Ossabaw pigs (Group I) at baseline and 4 months of C) LAD artery and D) LCX artery. The data is expressed as mean ± 1SD.

A comparison of lumen CSA measurements obtained from IVUS and CCTA showed similar results and trends for both methods [$p = 0.15$ at baseline (Fig. 4A) and $p = 0.11$ at 4 months (Fig. 4B) for LAD, and $p = 0.34$ at baseline (Fig. 4C) and $p = 0.06$ at 4 months (Fig. 4D) for LCX]. Hence, CCTA confirmed the IVUS findings of arterial enlargement. Fig. 5 shows the linear regression (Fig. 5A) and Bland–Altman (Fig. 5B) accuracy analysis for the IVUS lumen area vs. the CCTA lumen area. The mean difference between IVUS and CCTA was 0.06 ± 1.49 mm² (accuracy $p = $ NS).

The average percent stenosis determined by IVUS in Group I at 4 months was $2.2\% \pm 0.8\%$ (0 to 3.32%) over the length of the LAD, $1.6\% \pm 0.9\%$ (0 to 3.51%) for LCX, and $1\% \pm 0.8\%$ (0 to 1.94%) for RCA, as shown in Fig. 6A. The values were not statistically different in the three arteries. The percent stenosis in Group II at 12 months in the

LAD was $21.3\% \pm 14.2\%$, ranging from 0% to 61.3% (Fig. 6B). The results from Groups I and II were significantly different, $p = 0.03$. FFR values in Group I were within normal ranges at baseline (0.91 ± 0.07) and at 4 months (0.93 ± 0.05), $p = 0.71$, Fig. 6C.

To demonstrate the positive remodeling, we plotted the lumen area versus the percent stenosis at 12 months (Fig. 7). There was no significant relation between lumen CSA and percent stenosis below and above 35% stenosis (r values were 0.09 and 0.12, respectively), which confirms positive arterial remodeling.

4. Discussion

The major finding of this study was that Ossabaw pigs fed a high fat atherogenic diet developed diffuse coronary artery disease (DCAD) over
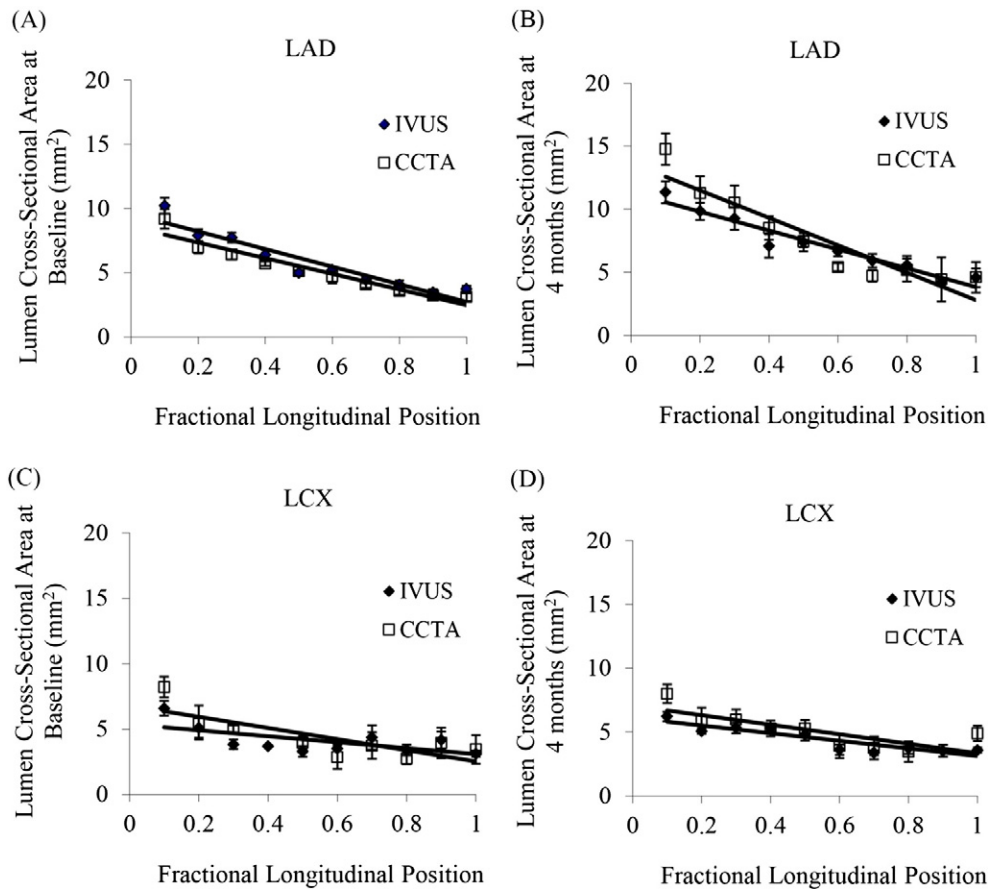
Fig. 4. Comparison of IVUS and CCTA measurements of LAD artery CSA at A) baseline and B) 4 months. Comparison of IVUS and CCTA measurements of LCX artery at C) baseline and D) 4 months. The data is expressed as mean ± 1SD.

time, and arterial positive remodeling (paradoxical increase in lumen area) during the early stages of the disease. Furthermore, after 12 months on atherogenic diet, a decrease in lumen CSA was observed, but it was still greater than that observed at baseline (Fig. 1A). Several studies [1–8] have shown arterial positive remodeling in the presence of focal disease but to our knowledge, this is the first report of a compensatory enlargement of the coronary arteries in a metabolic syndrome animal model with DCAD during the early stages of the disease.

The Ossabaw swine develop metabolic syndrome when fed an excess calorie atherogenic diet over several months [19]. All the pathological aspects of the animals' metabolic syndrome (hypertension, dyslipidemia, glucose intolerance, endothelial dysfunction, steatohepatitis, as well as atherosclerosis in the coronary vasculature) have been extensively described by several investigators [15,19,22,23]. Furthermore, the Ossabaw swine model of metabolic syndrome also develops mature, clinically significant atheroma with lipid cores, foam cells, proliferating smooth muscle cells, and small foci of calcification [15,24,25].

Positive remodeling is the mechanism by which the lumen CSA of arteries is preserved despite the development of atherosclerotic disease. The phenomenon was first described in human histopathologic specimens 25 years ago by Glagov and colleagues [2]. The investigators also reported that arterial enlargement occurred in relation to plaque burden (33.3%, mean) and that lumen stenosis was not present until the plaque occupied 40% of the lumen CSA [2]. Further accumulation of plaque resulted in decrease of lumen area. Since then, several studies have demonstrated the "Glagov phenomenon" in coronary arteries [1, 3] and peripheral arteries [8] of patients undergoing IVUS [1,3,8] or CCTA [6]. It has been suggested [26] that the increase in lumen CSA is largely compensatory; i.e., an adaptation to thickness of the intima to preserve vessel function.

Arterial vessels enlarge in response to a number of factors like body weight or heart size [26], age [27], and blood flow [28,29]. The mechanisms by which coronary arteries increase their lumen size in the presence of atherosclerosis remain unclear. Arterial enlargement may develop as a result of intimal plaque causing involution of the media with outward bulging of the lesion [29]. Bond et al. [30] observed substantial destruction of the tunica media, with dissolution of the internal elastic lamina and loss of smooth muscle cells. Armstrong et al. [26] noted diffuse thickening of the intima and focal atrophy and focal thinning of the media, albeit the total medial mass was not decreased. The degradation of mural connective tissue fibers by enzymes released by plaque cells has also been suggested as a contributing factor [2]. de Groot and Veldhuizen [31] have suggested the existence of a diffuse complex of changes that start with a gradual enlargement of the vessel followed by narrowing, with associated changes in the intima, media and adventitia.

Wall shear stress (WSS) can be estimated by Poiseuille's law, which states that shear stress is proportional to flow viscosity and inversely proportional to the third power of the internal radius [32]. Arterial lumen enlargement has been shown to occur in response to long-term increase in flow velocity and to continue until a normal level of WSS is restored [32,33]. The narrowing of the lumen caused by intimal hyperplasia or plaque deposition tends to increase flow velocity and WSS, which stimulates endothelial-dependent arterial dilation. Since flow did not change in our study and the lesions were fairly minor (<5% stenosis and normal FFR), the shear stress effect was likely not important in this study.
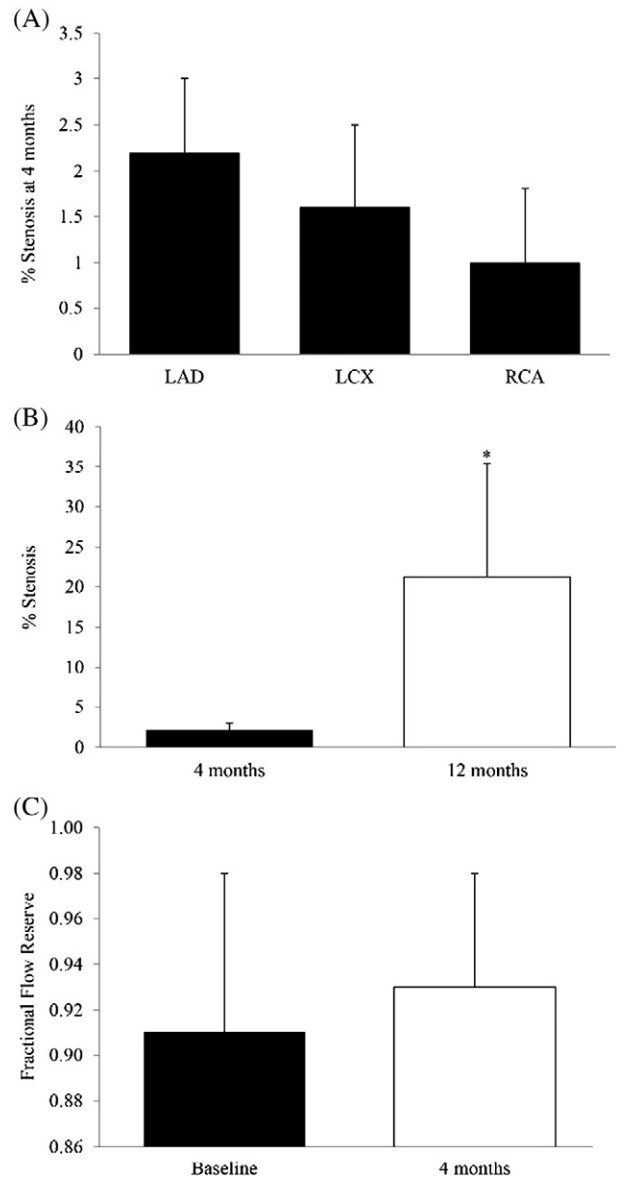
It has also been demonstrated [34] that a decrease in blood viscosity at a constant flow rate leads to arterial narrowing, whereas an increase in blood viscosity causes arterial enlargement. Although we did not
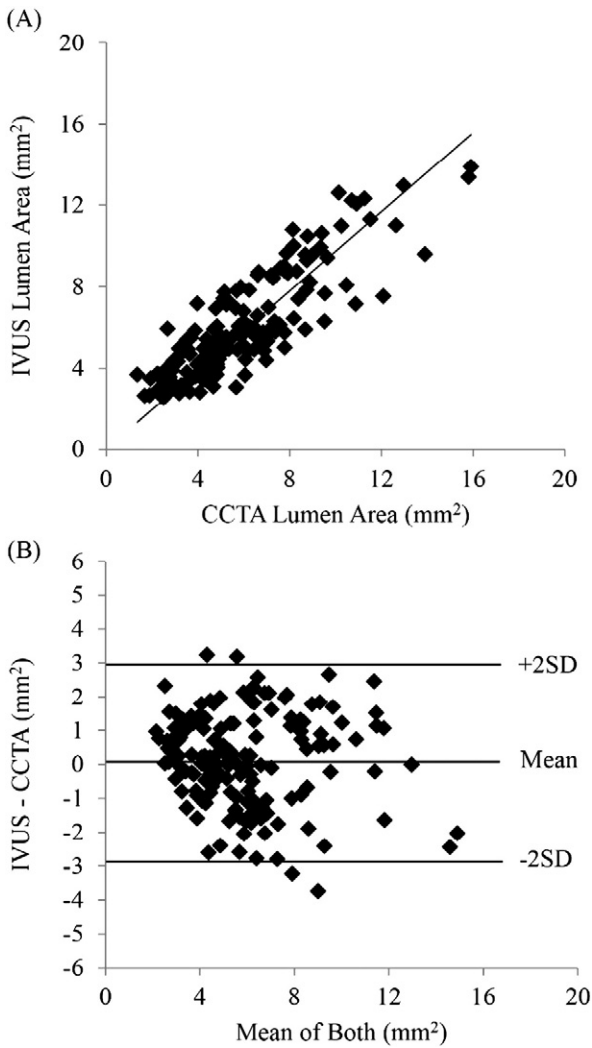
Fig. 5. A) Linear regression analysis between IVUS lumen area and CCTA lumen area; $R^2 = 0.68$. B) Bland–Altman accuracy analysis between both imaging modalities; mean of difference $= 0.06$ mm^2, $+2SD = 2.97$ mm^2, $-2SD = 2.85$ mm^2.

Fig. 6. A) Percent stenosis of LAD, LCX and RCA at 4 months of atherogenic diet (Group I). B) Percent stenosis of LAD artery at 4 (Group I) and 12 months (Group II) of atherogenic diet. C) FFR at baseline and at 4 months (Group I). The data is expressed as mean $\pm$ 1SD.

measure blood viscosity in this study, it is well known that viscosity is increased in animals fed with an atherogenic diet [35] and in hypercholesterolemic patients [36]. The increase in blood viscosity previously reported varies from 0.8% to 8.2% [37–39]. In hemodynamic studies of early atherosclerotic changes [26], vascular resistance was found to be increased in the resting state and also during maximal vasodilation. The greater viscosity of hypercholesterolemic blood may contribute to this finding, since lumen area is maintained or even increased. If we assume a 10% increase in blood viscosity in these animals, then a 3% increase in diameter would be expected to maintain uniform shear stress. Clearly, the increase in lumen CSA found in this study (mean of 25%) cannot be explained by the increase in viscosity, and hence, WSS.

In longitudinal animal studies, the enlargement of coronary arteries can be attributed to animal growth and differences in body weight. Atherosclerotic progression and regression experiments [26,30], however, have demonstrated that animals fed an atherogenic diet had much larger coronary arteries as compared to control groups, suggesting that in growing animals, atherosclerosis results in increased arterial size. The mean heart weights in our study were 183 g and 228 g at baseline and at 4 months, respectively. Given that CSA is proportional to M$^{2/3}$ [40], an approximately 15.7% increase in CSA would be expected. Hence, the greater lumen CSA found in this study cannot be attributed to animal and heart growth alone. Finally, diabetes mellitus, race, and sex are also minor determinants of artery size, while hypertension and cigarette smoking seems to have no independent influence on vessel size [29].

The differential degree of lumen remodeling in the three major coronary arteries is interesting. The IVUS studies suggest a greater increase in lumen CSA in the order of RCA > LAD > LCX. This was supported by the CT images, which suggest LAD > LCX. This may depend on the degree to which the vessel is supported by surrounding myocardium. The RCA tends to be most superficial and transverses along the base without penetrating into the myocardium, unlike the LAD and LCX. Hence, the RCA may be less restricted to expand radially due to the lack of myocardial restraint. The effect of surrounding tissue has clearly been shown to affect remodeling of vessels during pressure-overload [41].

Finally, positive coronary arterial remodeling has also been associated with stent malapposition after drug-eluting stent implantation [42]. Several studies have reported that positive remodeling was the main cause of late-acquired incomplete apposition, which was also associated with late and very late stent thrombosis [43–45].
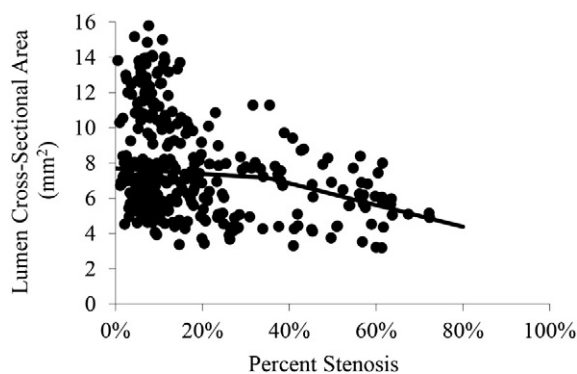
Fig. 7. Lumen area versus percent stenosis from seven Ossabaw pigs (Group II) after 12 months of atherogenic diet.

In conclusion, progression of coronary artery disease is typically associated with a compensatory enlargement of the vessel cross-sectional area, which results in paradoxical lumen expansion, at the earlier stages of atherosclerosis. The confirmation of the Glagov phenomenon in the Ossabaw animal model will lend to studies that may yield important new insights for the diagnosis, prevention and treatment of ischemic heart disease, especially for patients with metabolic syndrome, in whom there is a strong association with plaque vulnerability [46].

4.1. Study limitations

This study was designed to evaluate the remodeling process induced by the atherogenic diet up to 8 months. Unfortunately, animals developed cardiac arrest during CCTA imaging at 8 months, precluding us from obtaining additional longitudinal data beyond 4 months. Ossabaw pigs on an atherogenic diet are well known to be more susceptible to myocardial infarction as compared to domestic pigs. Hence, we considered a separate group of Ossabaw at 12 months. Although the measurements at 12 months were made in a different group of animals, their weights were similar at the beginning of the study, and both groups were fed the same atherogenic diet. Furthermore, two independent investigators analyzed the baseline and 4 months and the 12 months data, respectively.

Body weight-matched Yorkshire domestic pigs were used as the control group because Ossabaw miniature pigs do not grow or gain body weight when they are fed a lean diet. Compared with the lean domestic Yorkshire pig, the lean Ossabaw grows more slowly and has less muscle mass. The Yorkshire pigs have greater cellularity and cell size in the skeletal muscle. Subcutaneous fat thickness is at least twofold greater in obese Ossabaw pigs than in Yorkshire. Ossabaw obese pigs are not hyperglycemic or hyperinsulinemic relative to the lean Yorkshire but they do have reduced glucose tolerance and lower plasma growth hormone [47]. Despite the use of different species in this study, the differences in coronary anatomy are not expected to be significant and the positive remodeling in the distal coronary arteries (3–4 cm distal of main branch) is apparent (Fig. 2).

IVUS and CCTA imaging are limited by difficulties in matching single CSA at different time points. Although every effort was made to match the sites at baseline and at 4 months, matching may be imperfect at some points. We used the arterial branches as reference points, and normalized the data according to fractional longitudinal position for both methods. Finally, this atherosclerosis progression study only evaluated the atherosclerotic changes in coronary arteries for a relatively short period of time.

Although some studies using multislice CT angiography have failed to provide positive results in the primary prevention settings, new advances in imaging technology and computational sciences may allow the development of patient-specific models of coronary artery disease to accurately predict and prevent future cardiac events.

4.2. Significance

This is the first atherosclerosis progression study to demonstrate enlargement of the coronary arteries in a metabolic syndrome animal model with diffuse disease. Positive remodeling may represent an early marker of disease and an indication of future adverse events especially in patients with metabolic syndrome. Subjects with metabolic syndrome usually have multivessel involvement, more positive remodeling, and non-calcified plaques than those without metabolic syndrome. Positive remodeling in the early stages of coronary atherosclerosis often results in plaque rupture and acute events due to the higher lipid content and macrophage count in these plaques [48], thus requiring an accurate diagnosis. A better understanding of these findings should provide direction for the development of new algorithms to improve detection and management of coronary artery disease.

Conflict of interest

The authors report no relationships that could be construed as a conflict of interest.

Acknowledgments

References

[1] Ge J, Erbel R, Zamorano J, Koch L, Kearney P, Görge G, et al. Coronary artery remodeling in atherosclerotic disease: an intravascular ultrasonic study in vivo. Coron Artery Dis 1993;4(11):981–6.

[2] Glagov S, Weisenberg E, Zarins CK, Stankunavicius R, Kolettis GJ. Compensatory enlargement of human atherosclerotic coronary arteries. N Engl J Med 1987;316(22):1371–5.

[3] Hermiller JB, Tenaglia AN, Kisslo KB, Phillips HR, Bashore TM, Stack RS, et al. In vivo validation of compensatory enlargement of atherosclerotic coronary arteries. Am J Cardiol 1993;71(8):665–8.

[4] McPherson DD, Sirna SJ, Hiratzka LF, Thorpe L, Armstrong ML, Marcus ML, et al. Coronary arterial remodeling studied by high-frequency epicardial echocardiography: an early compensatory mechanism in patients with obstructive coronary atherosclerosis. J Am Coll Cardiol 1991;17(1):79–86.

[5] Nissen SE, Gurley JC, Grines CL, Booth DC, McClure R, Berk M, et al. Intravascular ultrasound assessment of lumen size and wall morphology in normal subjects and patients with coronary artery disease. Circulation 1991;84(3):1087–99.

[6] Rinehart S, Qian Z, Vazquez G, Joshi PH, Kirkland B, Bhatt K, et al. Demonstration of the Glagov phenomenon in vivo by CT coronary angiography in subjects with elevated Framingham risk. Int J Cardiovasc Imaging 2012;28(6):1589–99.

[7] Tobis JM, Mallery J, Mahon D, Lehmann K, Zalesky P, Griffith J, et al. Intravascular ultrasound imaging of human coronary arteries in vivo. Analysis of tissue characterizations with comparison to in vitro histological specimens. Circulation 1991;83(3):913–26.

[8] Losordo DW, Rosenfield K, Kaufman J, Pieczek A, Isner JM. Focal compensatory enlargement of human arteries in response to progressive atherosclerosis. In vivo documentation using intravascular ultrasound. Circulation 1994;89(6):2570–7.

[9] Asakura T, Karino T. Flow patterns and spatial distribution of atherosclerotic lesions in human coronary arteries. Circ Res 1990;66(4):1045–66.

[10] Sacks FM, Pasternak RC, Gibson CM, Rosner B, Stone PH. Effect on coronary atherosclerosis of decrease in plasma cholesterol concentrations in normocholesterolaemic patients. Harvard Atherosclerosis Reversibility Project (HARP) Group. Lancet 1994;344(8931):1182–6.

[11] Coskun AU, Yeghiazarians Y, Kinlay S, Clark ME, Ilegbusi OJ, Wahle A, et al. Reproducibility of coronary lumen, plaque, and vessel wall reconstruction and of endothelial shear stress measurements in vivo in humans. Catheter Cardiovasc Interv 2003;60(1):67–78.

[12] Malek AM, Alper SL, Izumo S. Hemodynamic shear stress and its role in atherosclerosis. JAMA 1999;282(21):2035–42.

[13] Stone PH, Coskun AU, Kinlay S, Clark ME, Sonka M, Wahle A, et al. Effect of endothelial shear stress on the progression of coronary artery disease, vascular remodeling, and in-stent restenosis in humans: in vivo 6-month follow-up study. Circulation 2003;108(4):438–44.

[14] Girerd X, London G, Boutouyrie P, Mourad JJ, Safar M, Laurent S. Remodeling of the radial artery in response to a chronic increase in shear stress. Hypertension 1996; 27(3 Pt 2):799–803.

[15] Neeb ZP, Edwards JM, Alloosh M, Long X, Mokelke EA, Sturek M. Metabolic syndrome and coronary artery disease in Ossabaw compared with Yucatan swine. Comp Med 2010;60(4):300–15.

[16] Guide for the care and use of laboratory animals. National Research Council (US) Committee for the update of the guide for the care and use of laboratory animals8th ed. . Washington (DC): National Academies Press (US); 2011.

[17] Cardon AD, Bailey MR, Bennett BT. The Animal Welfare Act: from enactment to enforcement. J Am Assoc Lab Anim Sci 2012;51(3):301–5.

[18] Lee L, Alloosh M, Saxena R, Van Alstine W, Watkins BA, Klaunig JE, et al. Nutritional model of steatohepatitis and metabolic syndrome in the Ossabaw miniature swine. Hepatology 2009;50(1):56–67.

[19] Dyson MC, Alloosh M, Vuchetich JP, Mokelke EA, Sturek M. Components of metabolic syndrome and coronary artery disease in female Ossabaw swine fed excess atherogenic diet. Comp Med 2006;56(1):35–45.

[20] Wischgoll T, Choy JS, Ritman EL, Kassab GS. Validation of image-based method for extraction of coronary morphometry. Ann Biomed Eng 2008;36(3):356–68.

[21] Paolo Cignoni, Marco Callieri, Massimiliano Corsini, Matteo Dellepiane, Fabio Ganovelli, Guido Ranzuglia. MeshLab: an open-source mesh processing tool. Sixth Eurographics Italian Chapter Conference; 2008 129–36.

[22] Sturek M, Alloosh M, Wenzel J, Byrd JP, Edwards JM, Lloyd PG, et al. Ossabaw Island miniature swine: cardiometabolic syndrome assessment. Swine in the laboratory: surgery, anesthesia, imaging, and experimental techniques. Boca Raton, FL: CRC Press; 2007. p. 397–402.

[23] Kreutz RP, Alloosh M, Mansour K, Neeb Z, Kreutz Y, Flockhart DA, et al. Morbid obesity and metabolic syndrome in Ossabaw miniature swine are associated with increased platelet reactivity. Diabetes Metab Syndr Obes 2011;4:99–105.

[24] Langohr IM, HogenEsch H, Stevenson GW, Sturek M. Vascular-associated lymphoid tissue in swine (Sus scrofa). Comp Med 2008;58:168–73.

[25] Wang HW, Langohr IM, Sturek M, Cheng JX. Imaging and quantitative analysis of atherosclerotic lesions by CARS-based multimodal nonlinear optical microscopy. Arterioscler Thromb Vasc Biol 2009;29:1342–8.

[26] Armstrong ML, Heistad DD, Marcus ML, Megan MB, Piegors DJ. Structural and hemodynamic response of peripheral arteries of macaque monkeys to atherogenic diet. Arteriosclerosis 1985;5(4):336–46.

[27] Hort W, Lichti H, Kalbfleisch H, Köhler F, Frenzel H, Milzner-Schwarz U. The size of human coronary arteries depending on the physiological and pathological growth of the heart, the age, the size of the supplying areas and the degree of coronary sclerosis. Virchows Arch A Pathol Anat Histol 1982;397(1):37–59.

[28] Rossitti S, Svendsen P. Shear stress in cerebral arteries supplying arteriovenous malformations. Acta Neurochir (Wien) 1995;137(3–4):138–45.

[29] Zarins CK, Weisenberg E, Kolettis G, Stankunavicius R, Glagov S. Differential enlargement of artery segments in response to enlarging atherosclerotic plaques. J Vasc Surg 1988;7(3):386–94.

[30] Bond MG, Adams MR, Bullock BC. Complicating factors in evaluating coronary artery atherosclerosis. Artery 1981;9(1):21–9.

[31] de Groot P, Veldhuizen RW. Human coronary artery remodeling, beginning and end of the atherosclerotic process. PLoS One 2006;1:e91.

[32] Kamiya A, Togawa T. Adaptive regulation of wall shear stress to flow change in the canine carotid artery. Am J Physiol 1980;239(1):H14–21.

[33] Zarins CK, Zatina MA, Giddens DP, Ku DN, Glagov S. Shear stress regulation of artery lumen diameter in experimental atherogenesis. J Vasc Surg 1987;5(3):413–20.

[34] Melkumyants AM, Balashov SA, Khayutin VM. Endothelium dependent control of arterial diameter by blood viscosity. Cardiovasc Res 1989;23(9):741–7.

[35] Amico-Roxas M, Drago F, Canonico PL, Russo A, Terranova R, Spitaleri A, et al. Plasma viscosity: relation to age, atherogenic diet and suloctidil. Pharmacol Res Commun 1981;13(8):765–7.

[36] Ercan M, Konukoglu D, Erdem Yeşim T. Association of plasma viscosity with cardiovascular risk factors in obesity: an old marker, a new insight. Clin Hemorheol Microcirc 2006;35(4):441–6.

[37] Solá E, Vayá A, Simó M, Hernández-Mijares A, Morillas C, España F, et al. Plasma viscosity and blood viscosity in obesity. Relationship with insulin resistance. Clin Hemorheol Microcirc 2007;37(4):309–18.

[38] Lowe GD, Drummond MM, Lorimer AR, Hutton I, Forbes CD, Prentice CR, et al. Relation between extent of coronary artery disease and blood viscosity. Br Med J 1980; 280(6215):673–4.

[39] Zhu W, Li M, Huang X, Neubauer H. Association of hyperviscosity and subclinical atherosclerosis in obese schoolchildren. Eur J Pediatr 2005;164(10):639–45.

[40] Choy JS, Kassab GS. Scaling of myocardial mass to flow and morphometry of coronary arteries. J Appl Physiol 2008;104(5):1281–6.

[41] Choy JS, Dang Q, Molloi S, Kassab GS. Nonuniformity of axial and circumferential remodeling of large coronary veins in response to ligation. Am J Physiol Heart Circ Physiol 2006;290(4):H1558–65.

[42] Finn AV, Nakazawa G, Joner M, Kolodgie FD, Mont EK, Gold HK, et al. Vascular responses to drug eluting stents: importance of delayed healing. Arterioscler Thromb Vasc Biol 2007;27(7):1500–10.

[43] Hong MK, Mintz GS, Lee CW, Park DW, Park KM, Lee BK, et al. Late stent malapposition after drug-eluting stent implantation: an intravascular ultrasound analysis with long-term follow-up. Circulation 2006 Jan 24;113(3):414–9.

[44] Cook S, Ladich E, Nakazawa G, Eshtehardi P, Neidhart M, Vogel R, et al. Correlation of intravascular ultrasound findings with histopathological analysis of thrombus aspirates in patients with very late drug-eluting stent thrombosis. Circulation 2009; 120(5):391–9.

[45] Hassan AK, Bergheanu SC, Stijnen T, van der Hoeven BL, Snoep JD, Plevier JW, et al. Late stent malapposition risk is higher after drug-eluting stent compared with bare-metal stent implantation and associates with late stent thrombosis. Eur Heart J 2010;31(10):1172–80.

[46] Zheng M, Choi SY, Tahk SJ, Lim HS, Yang HM, Choi BJ, et al. The relationship between volumetric plaque components and classical cardiovascular risk factors and the metabolic syndrome a 3-vessel coronary artery virtual histology-intravascular ultrasound analysis. JACC Cardiovasc Interv 2011;4(5):503–10.

[47] Hunt CE, Hunt CE. Metabolic disorders — obesity. Spontaneous animal models of human disease. New York, NY: Academic Press, Inc; 1979. p. 78–9.

[48] Varnava AM, Mills PG, Davies MJ. Relationship between coronary artery remodeling and plaque vulnerability. Circulation 2002;105(8):939–43.